Limits of Chromosome Compaction by Loop-Extruding Motors

Edward J. Banigan[1,2,*] and Leonid A. Mirny[1,2,†]

[1]*Institute for Medical Engineering and Science, Massachusetts Institute of Technology, Cambridge, Massachusetts 02139, USA*

[2]*Department of Physics, Massachusetts Institute of Technology, Cambridge, Massachusetts 02139, USA*

(Received 4 December 2018; revised manuscript received 18 February 2019; published 11 July 2019)

During mitosis, human chromosomes are linearly compacted about 1000-fold by loop-extruding motors. Recent experiments have shown that condensins extrude DNA loops but in a "one-sided" manner. This contrasts with existing models, which predict that symmetric, "two-sided" loop extrusion accounts for mitotic chromosome compaction. We explore whether one-sided extrusion, as it is currently seen in experiments, can compact chromosomes by developing a mean-field theoretical model for polymer compaction by motors that actively extrude loops and dynamically turnover. The model establishes a stringent upper bound of only about tenfold for compaction by strictly one-sided extrusion. We confirm this result with stochastic simulations. Thus, strictly one-sided extrusion as it has been observed so far cannot be the sole mechanism of chromosome compaction. However, as shown by the model, other two-sided or effectively two-sided mechanisms can achieve sufficient compaction.

DOI: 10.1103/PhysRevX.9.031007

Subject Areas: Biological Physics, Interdisciplinary Physics, Soft Matter

Chromosomes are exceedingly long polymers of chromatin, i.e., DNA and associated proteins. Each chromosome in a human cell is comprised of about 1 mm of chromatin, which is dynamically reorganized throughout the cell cycle. During mitosis, chromosomes are linearly compacted about 1000-fold, forming about 1–5-μm-long cylindrical shapes. This compaction is achieved by the formation of an array of chromatin loops [1–8] [Fig. 1(a)]. While proteins that are essential for this process are known [9–11], the physical mechanisms underlying this dramatic compaction are not fully understood.

The protein complex condensin has been shown to be both necessary and sufficient for mitotic chromosome compaction [8–14], but the molecular mechanism by which it performs this task remains unknown. It has been hypothesized [15–17] that condensin and other SMC (structural maintenance of chromosomes) complexes are molecular motors that actively extrude chromatin loops through a yet to be discovered mechanism [18,19]. These loop-extruding factors (LEFs) load onto the chromatin fiber and progressively form larger loops by reeling chromatin into the loops [Fig. 1(b)]. Models suggest that loop extrusion can dynamically generate various chromosome structures [7,20–26], including linearly compacted mitotic chromosomes. Experiments support loop extrusion as a common phenomenon in living cells [7,8,27–41], but this motor activity had not been directly observed until recently.

Recent *in vitro* single-molecule experiments demonstrated that yeast condensins actively extrude DNA loops in an ATP-dependent manner [42], supporting the loop-extrusion mechanism. However, loop extrusion in these experiments was one-sided, so that the DNA on only one side of the condensin was reeled into the loop [Fig. 1(c)]. This conflicts with previous models, which assumed that each LEF consists of two connected motors that reel chromatin from both sides and thus performs "two-sided" extrusion [Fig. 1(b)]. Thus, these experiments raise the question of whether one-sided extrusion can also generate the chromosome structures attributed to loop extrusion, particularly linearly compacted mammalian chromosomes.

More generally, translocating molecular motors, such as those found in the cytoskeleton, can exhibit a variety of collective effects, depending on motor kinetics and directionality, among other properties [43,44]. Previous work has shown that microscopic changes in the mode of motor activity along a polymer chain (e.g., chromatin) can lead to large-scale changes in polymer structure and dynamics [45,46]. Indeed, a common feature of active systems is that their emergent behaviors are controlled by the underlying symmetries of their individual components [47–49].

*ebanigan@mit.edu
†leonid@mit.edu

Published by the American Physical Society under the terms of the Creative Commons Attribution 4.0 International license. Further distribution of this work must maintain attribution to the author(s) and the published article's title, journal citation, and DOI.

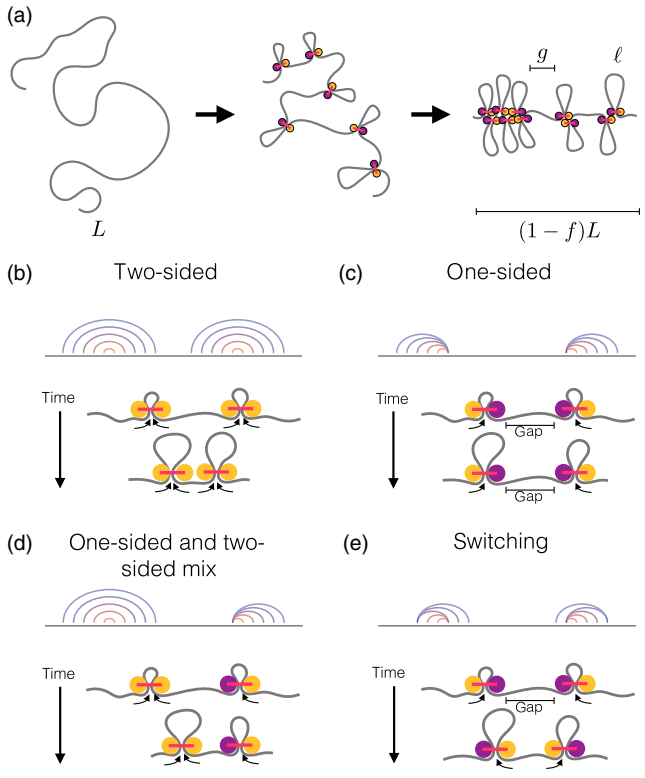

FIG. 1. (a) Linear compaction of chromatin polymer by LEFs. LEFs progressively compact the polymer from its initial length L. In steady state, the polymer is $\mathcal{FC}$-fold compacted into a dynamic loop array with a backbone of length $(1-f)L$. Uncompacted gaps of average size g containing polymer that has not been extruded may remain between loops of size ℓ. (b) Top: Arch diagram showing positions of two two-sided LEFs at different times, with time indicated by color from red (early) to blue (late). Bottom: Drawing of two-sided LEFs (yellow and pink) translocating along chromatin/DNA (gray) and progressively growing loops. (c) Arch diagram with time progression of one-sided LEF positions and drawing of one-sided LEFs, each with its inactive head shown in purple. LEFs in the depicted configuration leave an unextruded gap. (d) A mixture of one- and two-sided LEFs. (e) One-sided LEFs that switch which side extrudes can eliminate initially unextruded gaps if at least one of the LEFs switches.

However, only a few theoretical studies have addressed the unique situation of loop extrusion, in which motors effectively translocate by extruding their polymer substrate. Moreover, existing theoretical models cannot easily be extended to consider asymmetric loop extrusion [17,21].

To investigate the ability of condensin to compact chromosomes, we develop a mean-field theoretical model using the minimal set of condensin properties observed in experiments to date. In the model, LEFs load uniformly onto DNA and continuously extrude loops in a directed manner; they dissociate with exponentially distributed lifetimes. LEFs do not interact except by acting as barriers to extrusion by other LEFs if they are adjacent. We consider the cases of two-sided LEFs [Fig. 1(b)], one-sided LEFs [Fig. 1(c)], a mix of one- and two-sided LEFs [Fig. 1(d)], and one-sided LEFs that can switch which side extrudes [Fig. 1(e)]. For these cases, we predict upper limits for linear compaction, which we measure as the contour length of the fully extended polymer compared to the length of the backbone of the folded polymer [Fig. 1(a) and Eq. (1)]. Surprisingly, pure one-sided loop extrusion can achieve only up to tenfold compaction, even with LEF turnover. While this may be sufficient for yeast chromosomes [50], it cannot be the mechanism underlying the approximately 1000-fold compaction of mammalian mitotic chromosomes. Thus, the model establishes a general physical rule for linear folding of polymers such as chromatin: Dramatic compaction requires locally bidirectional activity.

We model LEFs as two-headed complexes with either one or two active heads [Figs. 1(b) and 1(c)]. Each active head directionally translocates along a continuous chromatin/DNA polymer at speed v in one dimension, modeling *in vitro* observations of directed motion [42,51]. For one-sided extrusion, one head is inactive and stationary [42], and only the active head reels chromatin into the extruded loop, which grows at speed v. For two-sided extrusion, both heads are active, and the loop grows at speed $2v$. To model condensin loading and unloading dynamics [51–54], LEFs stochastically bind chromatin at rate k_b and unbind at rate k_u, leading to a steady-state average of $N_b = k_b N/(k_u + k_b)$ of polymer-bound LEFs, where N is the total number of LEFs in the system. A LEF may load within an existing loop, thus forming a *child* loop that either splits or reinforces the *parent* loop [Fig. 2(a)]. Loops formed by LEFs stochastically appear, grow, shrink, and vanish in the dynamic steady state.

As shown for two-sided extrusion [21], two length scales control the dynamics of the system: LEF processivity, $\lambda = 2v/k_u$, i.e., the average size of a loop formed by an unobstructed LEF; and the average separation, $d = L/N_b$, of LEFs on the polymer. For $d \gg \lambda$, LEFs are sparse; thus, they do not obstruct each other and rarely nest, and the polymer is not significantly compacted. In contrast, $d \ll \lambda$ is a dense regime in which most of the polymer is extruded into reinforced loops, which yields high (>500-fold) linear compaction. For two-sided extrusion in this regime, the entire polymer can be extruded into loops because extrusion eliminates all gaps between loops. One-sided extrusion, however, unavoidably leaves gaps between LEFs, leading to incomplete compaction.

To examine compaction by one-sided extrusion, we consider possible orientations of neighboring one-sided LEFs. In three of four possible configurations, one-sided LEFs can close the gap between them if they remain bound to the polymer for a sufficiently long time. In the remaining configuration, adjacent LEFs necessarily leave a gap between them because the intervening polymer is not extruded by either LEF [Fig. 2(b)]. Thus, in the dense regime ($\lambda/d \gg 1$), where extrusion is much faster than

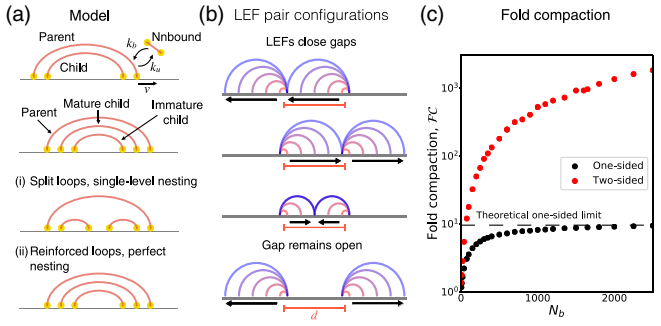

FIG. 2. (a) Top half: A parent LEF is associated with chromatin at the base of an extruded loop, and a child LEF is associated within the loop. A bound LEF can unbind chromatin to become an unbound LEF, and an unbound LEF can bind to become a parent or child. A mature child LEF will become a parent LEF if the current parent LEF unbinds, while a more deeply nested "immature" child LEF would remain a child. Bottom half: Loop nesting architectures. With (i) single-level nesting, child LEFs split parent loops, while with (ii) perfect nesting, child LEFs reinforce the parent loops. (b) Possible configurations of pairs of adjacent one-sided LEFs, each shown at different times indicated by color from red (early) to blue (late). The side of extrusion (and direction of motor translocation) is indicated by arrows. The one configuration in which active LEF subunits translocate away from each other by extruding chromatin from opposite sides of the polymer leaves a gap. (c) Simulation results for fold compaction $\mathcal{FC}$ by one-sided extrusion (black) and two-sided extrusion (red), shown for varying number of bound LEFs, N_b.

exchange kinetics, one-sided LEFs segment chromatin into N_p parent loops and $N_p/4$ gaps between the loops.

To calculate the maximum fold compaction ($\mathcal{FC}$) achievable by one-sided LEFs, we consider the maximum compacted fraction f, defined as the fraction of the polymer extruded into loops. These quantities are related as

$$\mathcal{FC} = 1/(1-f). \tag{1}$$

Note that $\mathcal{FC}$ measures the factor by which the length of the backbone of the compacted polymer is shorter than the fully extended polymer, provided that the mean loop size ℓ is less than the linear length of the compacted polymer's backbone, i.e., $\ell < (1-f)L$. This condition holds for sufficiently long polymers [55]. Thus, Eq. (1) shows that even a modest fraction, $1-f$, of unextruded polymer in gaps strictly limits the degree of linear compaction of the polymer.

We start by calculating mean loop and gap sizes. The LEFs segment chromatin of length L into parent loops of mean size,

$$\ell = fL/N_p, \tag{2}$$

and gaps with mean size equal to the mean distance between the loading sites of two adjacent LEFs [Fig. 2(b)],

$$g = d = L/N_b = L/(N_p + N_c), \tag{3}$$

where N_c is the number of child LEFs. A key assumption of the model is the existence of these unextruded gaps. As explained above, we expect gaps to occur for one of four LEF configurations [Fig. 2(b)], so a total of N_p parent loops and $N_p/4$ gaps cover the whole polymer:

$$N_p\ell + \frac{N_p}{4}g = L. \tag{4}$$

Combining Eqs. (2)–(4), we obtain the compacted fraction that has been extruded into loops:

$$f = \frac{4\ell}{4\ell + g} = 1 - \frac{N_p}{4(N_p + N_c)}. \tag{5}$$

This result indicates that significant lengthwise compaction by one-sided LEFs requires a large number of child LEFs per parent (e.g., $f = 0.99$, or $\mathcal{FC} = 100$, requires $N_c \approx 25N_p$).

To explore whether this picture can be altered by LEF turnover, we determine the steady-state kinetics of unbound, parent, and child LEFs. A new parent is formed if one of the N_u unbound LEFs binds to a chromosomal position that is not within an extruded loop. Alternatively, an unbound LEF becomes a child LEF if it binds to a site within an extruded loop [Fig. 2(a)]. Thus, assuming uniform loading along the polymer, upon binding, an unbound LEF becomes a child LEF with probability f or a parent LEF with probability $1-f$. Upon unbinding of a parent LEF, child LEFs previously nested within the parent loop may become parents if they are "mature," i.e., not nested within any loop other than the parent [Fig. 2(a)]. The average number of mature children per parent, denoted by α, depends on the loop nesting architecture. LEF kinetics are therefore described by

$$\begin{aligned}
\dot{N}_u &= k_u(N_p + N_c) - k_b N_u, \\
\dot{N}_p &= k_b(1-f)N_u - k_u N_p + \alpha k_u N_p, \\
\dot{N}_c &= k_b f N_u - k_u N_c - \alpha k_u N_p.
\end{aligned} \tag{6}$$

We assume that all rates are nonzero, so there is a well-defined nontrivial steady state that is independent of the initial configuration of loop extruders [56]. Moreover, we note that these equations implicitly assume exponentially distributed association and dissociation times for LEFs. Solving these equations in steady state yields a relation between the numbers of child and parent loops:

$$N_c = \frac{f-\alpha}{1-f}N_p. \tag{7}$$

This equation fixes the ratio of average numbers of child LEFs to parent LEFs for each possible f. Moreover, using Eq. (7) to substitute for N_c in Eq. (5), we find that the mean number of mature child loops per parent loop in steady state is $\alpha = 3/4$. However, to completely solve the system and

determine the maximum compaction f from Eq. (5), we still must determine the relationship between N_p and N_c.

To find the maximum possible compaction, we consider two limiting loop architectures: (i) single-level nesting in which all child LEFs are mature so that child LEFs only split parent loops, and (ii) perfect nesting in which each parent loop is reinforced by at most one mature child LEF, and each child LEF is reinforced by at most one child [Fig. 2(a)].

With single-level nesting, $\alpha = N_c/N_p = 3/4$, and each child LEF becomes a parent when its parent LEF unbinds [Fig. 2(a)i]. From Eq. (5), the maximum compaction is

$$f = 6/7 = 0.857. \tag{8}$$

We also find LEFs per parent loop, $(N_p + N_c)/N_p = 7/4$, and loop sizes, $\ell = fL/N_p = 3d/2$.

With perfect LEF nesting, each parent loop has at most one mature child [Fig. 2(a)ii]. We calculate the probability that a parent loop does not have a child in the limit of large N_p and N_c:

$$P(\text{no loops}) = (1 - 1/N_p)^{N_c} \approx e^{-N_c/N_p}. \tag{9}$$

The probability that a parent loop contains a child loop is thus $\alpha = 1 - e^{-N_c/N_p} = 3/4$, and we find

$$(N_p + N_c)/N_p = 1 + \ln 4 = 2.39. \tag{10}$$

Combining Eqs. (5) and (10), we find the compaction limit

$$f = \frac{3 + 4\ln 4}{4 + 4\ln 4} = 0.895, \tag{11}$$

or $\mathcal{FC} = 9.55$. Additionally, the mean loop size is

$$\ell = (1 + \ln 4) f d = 2.14 d. \tag{12}$$

In the dense regime ($\lambda/d \gg 1$), the mean distance between LEFs, $d = L/N$, controls the scaling behavior of the system. For instance, increasing the number of LEFs, N, decreases the gap size g as $1/N$, but it also increases the number of gaps, N_g, as N. As a result, the average total length of unextruded gaps, $N_g g$, is constant, fixing the maximum compacted fraction f [57]. Thus, one-sided extrusion (for both nesting architectures) achieves at most about tenfold compaction, along with small loops and little LEF nesting.

Importantly, Eq. (11) gives the maximum degree of chromatin compaction achievable by one-sided loop extrusion. To see that perfect nesting gives the upper bound to the maximum compaction [Eq. (11)] while single-level nesting corresponds to the lower bound [Eq. (8)], we rewrite Eq. (7) as

$$f = \frac{\alpha + N_c/N_p}{1 + N_c/N_p}. \tag{13}$$

This equation is an increasing function of N_c/N_p for $N_c/N_p > 0$. The two cases are the lower and upper bounds for N_c/N_p, and thus, the two extremes of possible loop architectures. They correspond to the bounds for the compaction limit; the compaction limits of all other architectures fall within the range defined by these extremes. Thus, we predict that chromosomes cannot be linearly compacted by more than an average of tenfold for any loop architecture generated by one-sided LEFs with independent kinetics.

To test the predictions of the mean-field theory, we use stochastic simulations to measure polymer compaction by one-sided LEFs in the dense regime ($\lambda/d \gg 1$). Adapting the simulation model in Ref. [21], we simulate N one-sided LEFs that extrude loops at speed v and have stochastic kinetics described by Eq. (6). In contrast to the theory, the simulated polymer is not continuous; rather, it is a chain of L discrete monomers. To avoid large finite-size effects, we consider a very long polymer such that the ratio L/d is large ($\approx 10^3$) [56]. This parameter choice is consistent with the ratio $L/d \approx 10^3$–10^4 expected for mammalian chromosomes [54,58,59].

The simulations confirm that the mean-field theory with perfect nesting accurately predicts the fraction compacted, f; for large λ/d, $f = 0.895$ ($\mathcal{FC} = 9.53$) in simulations [see large N_b in Fig. 2(c), $\phi = 0$ in Fig. 3(a), and Eq. (11)]. Moreover, the simulations illustrate the drastic decrease in fold compaction achievable with the minimalistic model for one-sided LEFs as compared with two-sided LEFs [Fig. 2(c)].

The simulations also confirm other predictions of the theoretical model. Given the possible configurations of LEFs [Fig. 2(b)], we expect one gap of size $g = d$, per four loops. In accordance with the theory, we observe $N_g/N_p = 0.22$ and mean gap size $g \approx d$ in the simulations (Fig. S1 [56]). Moreover, consistently with the theory ($\alpha = 3/4$), the number of mature child LEFs per parent LEF in steady-state simulations is $\alpha = 0.76$. We also observe $(N_p + N_c)/N_p = 2.13$ LEFs per loop [Eq. (10)] and a mean loop size of $\ell = 1.90d$ [Eq. (12)]. Differences in $(N_p + N_c)/N_p$ and ℓ between simulation and theory are due to the theoretical assumption of perfectly nested loops, which is violated by 18% of parent loops. Deviations in $(N_p + N_c)/N_p$ and ℓ offset each other when computing f; the theory predicts fewer but larger loops than observed in simulations. Altogether, the simulation results indicate that the mean-field theory accurately describes LEF dynamics, loop architecture, and maximum polymer compaction in the dense regime ($\lambda/d \gg 1$).

We have found that one-sided LEFs with the minimal properties observed in single-molecule experiments [42,51] are unable to achieve the dramatic polymer compaction

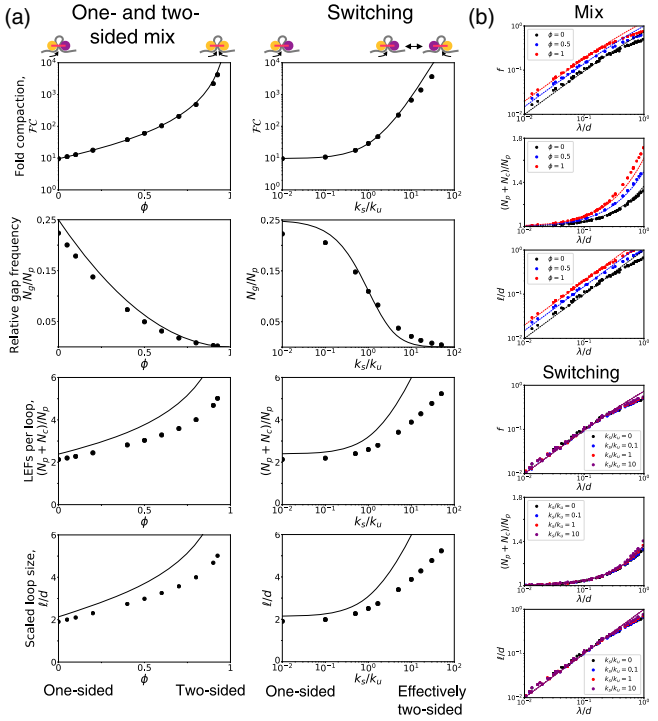

FIG. 3. (a) Simulation (points) and theory (lines) in the dense $\lambda/d \gg 1$ regime for models with a mix of one- and two-sided LEFs (left) and switching (right). From top to bottom: $\mathcal{FC}$, relative gap frequency (N_g/N_p), LEFs per loop [$(N_p+N_c)/N_p$], and scaled loop sizes (ℓ/d). Note that $\phi=0$ (or $k_s/k_u=0$) for pure one-sided extrusion, and $\phi=1$ (or $k_s/k_u\to\infty$) for (effectively) two-sided extrusion. (b) Fraction compacted (f), LEFs per loop, and scaled loop sizes in the sparse $\lambda/d<1$ regime.

needed to package mammalian mitotic chromosomes *in vivo* [4,5]. To explore how one-sided loop extrusion may nonetheless facilitate mitotic chromosome compaction, we extend the theory to identify variants of loop extrusion that can fully compact mitotic chromosomes.

We consider a model in which a fraction ϕ of the LEFs are two-sided and $1-\phi$ are one-sided [Fig. 1(d)]. Since two-sided LEFs can close all gaps, there is one configuration of LEFs that leaves a gap out of nine possible configurations. The frequency with which this configuration appears is $N_g/N_p=(1-\phi)^2/4$. The equation relating loops and gaps [previously, Eq. (4)] becomes

$$N_p\ell + N_p g(1-\phi)^2/4 = L, \tag{14}$$

so the compaction fraction in this model is given by

$$f = \frac{4\ell(1-\phi)^{-2}}{4\ell(1-\phi)^{-2}+g} = 1-\frac{N_p(1-\phi)^2}{4(N_p+N_c)}. \tag{15}$$

High compaction can be achieved with little LEF nesting when enough two-sided LEFs are present. For $\lambda/d \gg 1$, LEFs form reinforced loops [21], so we assume perfect nesting and note that $\alpha=(3+2\phi-\phi^2)/4$, to find

$$f = \frac{3+2\phi-\phi^2+4\ln\left(4(1-\phi)^{-2}\right)}{4+4\ln\left(4(1-\phi)^{-2}\right)}, \tag{16}$$

which is plotted in Fig. 3(a). The theory also predicts the LEFs per loop $(N_p+N_c)/N_p$, mean loop size ℓ, and number of gaps per loop, N_g/N_p, observed in simulations [Fig. 3(a), left]. The simulations show that the mean-field theory based on a predicted number of gaps per loop accurately captures the maximum compaction achievable by mixtures of one- and two-sided LEFs [Fig. 3(a)].

According to Eq. (16), a 1:1 mix of one- and two-sided LEFs yields $f=0.983$ or $\mathcal{FC}\approx 60$. Note that $\mathcal{FC}=100$ requires a fraction of $\phi=0.59$ two-sided LEFs, and $\mathcal{FC}=1000$ requires $\phi=0.84$. Thus, even a modest fraction of one-sided LEFs can perturb mitotic chromosome compaction. As expected for $\lambda/d \gg 1$, pure two-sided extrusion ($\phi=1$) yields 100% compaction. Thus, to eliminate unextruded gaps and fully compact chromosomes in this model, a large majority of the LEFs must be two-sided, which contrasts with current observations from *in vitro* experiments.

Therefore, we consider an alternative model in which one-sided LEFs close gaps without simultaneously extruding from both sides. Here, LEFs are instantaneously one-sided, but each LEF stochastically switches which side actively extrudes at rate k_s [Fig. 1(e)]. In principle, switching could occur due to the exchange of subunits of the SMC complex while the complex remains loaded [53], alterations to solution conditions [42], or post-translational or genetic modifications [60,61].

Compaction is limited by the degree to which the LEFs act in a purely one-sided manner. LEFs that switch before unloading can close adjacent gaps, regardless of the orientation of the adjacent LEFs, whereas LEFs that do not switch are effectively one-sided. We calculate the fraction n_2 of one-sided LEFs that switch before unloading by solving

$$\begin{aligned}\dot{n}_1 &= -(k_s+2k_u)n_1,\\ \dot{n}_2 &= k_s n_1,\end{aligned} \tag{17}$$

and finding $n_2 \equiv \lim_{t\to\infty} n_2$. In the $\dot{n}_1$ equation, $2k_u$ is used because in order for a LEF in a LEF pair to be effectively two-sided, it must switch before either it or its neighbor unbinds. The fraction of effectively two-sided LEFs is

$$n_2 = \frac{k_s/k_u}{2+k_s/k_u}. \tag{18}$$

This fraction only depends on k_s/k_u, the rate of switching compared to the unloading rate. For fast switching, $n_2\to 1$.

By substituting n_2 for the fraction ϕ of two-sided LEFs into Eq. (16), we find the compaction limit as a function of k_s/k_u:

$$f = 1-\frac{1}{(2+k_s/k_u)^2\left(1+2\ln(2+k_s/k_u)\right)}. \tag{19}$$

Again, the theory predicts values for the compaction limit, gaps per loop, LEFs per loop, and mean loop size that agree with simulation observations [Fig. 3(a), right].

Equation (19) indicates that a fast, but physiologically plausible, switching rate is required to achieve robust compaction. For example, $\mathcal{FC} = 100$ requires $k_s/k_u = 2.9$, while $\mathcal{FC} = 1000$ requires $k_s/k_u = 10.8$. The unloading rate k_u is observed to be of order 0.1 min^{-1} [51–54,62–64], so the expected switching rate is of order 1 min^{-1}. However, switching was not observed over 1–5 minutes of observations in recent *in vitro* single-molecule experiments [42]. Thus, LEF switching would require some as yet unknown *in vivo* factor or condition. Nonetheless, the theory and simulations indicate that effectively two-sided extrusion is required for 1000-fold linear compaction of mitotic chromosomes.

The theory can be extended to another physiologically important regime that is relevant to the SMC complex cohesin. While we have explored the dense ($\lambda/d \gg 1$) regime relevant to condensin-driven compaction of mitotic chromosomes, organization of interphase topologically associated domains (TADs) is likely driven by loop-extruding cohesins with $\lambda/d \lesssim 1$ [23,24,32–34]. Thus, we explore the sparse $\lambda/d < 1$ regime, in which LEFs leave unextruded gaps on both sides because LEF processivity is smaller than the distance between LEFs.

To compute compaction f, note that each loop grows unimpeded, and the loop size is the processivity; thus, $\ell \approx \lambda(1-\phi) + 2\lambda\phi$ (with $\lambda = v/k_u$ and $\phi = 0$ for the switching model since only one subunit is active at any time). We substitute for α in Eq. (7) and use $\ell = fL/N_p = fd(N_p + N_c)/N_p$. For both perfect nesting and single-level nesting, with small λ/d and f, we find [56]

$$f \approx (1+\phi)\lambda/d. \tag{20}$$

Simulations confirm this theoretical result [Fig. 3(b)]. Thus, for $\lambda/d \ll 1$, compaction is linear in λ/d, and loop nesting is unimportant because it is rare. This is true for both one- and two-sided extrusion in the sparse regime, but whether one-sided extrusion can organize chromosome structures such as interphase TADs in eukaryotes [27–34] remains unresolved.

Together, the theory and simulations show that the linear compaction of mitotic chromosomes is dependent on the ability of LEFs to eliminate uncompacted gaps between extruded loops. Thus, pure one-sided loop extrusion alone is unable to robustly compact chromosomes by more than tenfold [Figs. 2(c) and 3(a)] because it inevitably leaves one uncompacted gap for every four loops [Fig. 2(b)]. A stochastic, but steady, population of gaps (of mean size $g = d$) remains in the steady state of dynamically exchanging LEFs, and gaps cannot be eliminated merely by increasing the number of bound LEFs. Moreover, these gaps cannot be reliably eliminated if the "safety belt" that anchors each one-sided LEF [42,60] is released to allow free diffusion along DNA; gaps would not be eliminated because loop growth would be inhibited by loop conformational entropy [65]. We emphasize that the failure of pure one-sided loop extrusion to compact chromosomes is not strictly due to the simplicity of the model; the similarly simple two-sided extrusion model can easily achieve 1000-fold compaction [17,21]. Instead, compaction by one-sided extrusion is fundamentally limited by an intrinsic physical mechanism, the presence of unextruded gaps. The resulting tenfold linear compaction may be sufficient for yeast chromosomes [50], but it is inconsistent with *in vivo* observations of greater than 100-fold linear compaction of mammalian chromosomes [4,5].

Additional factors could be incorporated into the model, such as transcription [41,66] and internucleosome interactions, but it has already been established experimentally that robust chromatid compaction can be achieved with only condensins and a minimal set of purified components, among which histones are unnecessary [10,11]. Topoisomerase II, for example, is essential, but it does not directly compact chromatin; instead, it allows loop extrusion by condensin to overcome topological constraints [20,67,68]. Other factors may contribute to mitotic chromosome organization, but they either assist condensin activity [69] or are generally dispensable for compaction [10,11].

In principle, polymers could be compacted further by 3D attractive interactions between LEFs, but this would contradict a number of experimental observations. First, interactions sufficient to further compact chromosomes would lead to isotropic globular chromosomes [70–72], unlike what is observed *in vivo* (e.g., Refs. [6,12,54]). Second, 3D interactions are unlikely to preserve the linear ordering of loops [7,8,73] and may interfere with chromatid segregation [20,71,74]. Third, full compaction by 3D interactions may require large interaction energies and result in large clusters of LEFs [70,72], which are not seen *in vivo* [54].

Furthermore, 3D simulations indicate that without 3D interactions, polymers compacted by one-sided loop extrusion are isotropic random walks [65]. This result is expected from theoretical and computational studies of polymer "combs" [74–78], i.e., polymers with side chains (or here, loops) sparsely grafted to the main backbone. While repulsive interactions between loops could, in principle, induce rigidity and rodlike shapes by stretching the backbone, unextruded gaps limit the average grafting density and the gaps are flexible segments. Thus, the polymer has an isotropic random walk structure. Moreover, it has been shown that polymer combs with strong 3D attractive interactions (i.e., poor solvent) undergo an isotropic collapse (volumetric compaction) via a coil-globule transition [79,80]. Thus, we conclude that 3D attractive interactions and one-sided loop extrusion together are not sufficient to generate mitotic chromosomes.

A possible explanation of our findings is that yeast condensins, which were used in single-molecule experiments, are one-sided extruders as observed *in vitro*

[42], while mammalian condensins are two-sided. Yeast chromosomes are of order 1 megabase pair (Mbp), so they may require less compaction than human chromosomes, which are of order 100 Mbp. To quantitatively compare these cases, note that 1 bp = 0.34 nm and DNA has persistence length $\ell_p = 50$ nm (note that a similar argument holds if we consider a chromatin fiber with nucleosomes [81]). We expect uncompacted 3D chromosome lengths of

$$R_{\text{yeast}} \approx (10^6/150)^{1/2}(50\text{ nm}) \approx 4\ \mu\text{m},$$
$$R_{\text{human}} \approx (10^8/150)^{1/2}(50\text{ nm}) \approx 40\ \mu\text{m}. \quad (21)$$

Thus, tenfold linear compaction, which reduces the contour length of the chromosome's polymer backbone by a factor of 10, may reduce the 3D size by a factor of $\sqrt{10} \approx 3$. This reduction would produce micron-sized yeast chromosomes but 10-micron human chromosomes. Thus, yeast chromosomes require only a few-fold linear compaction, while human chromosomes need more than 100-fold linear compaction for 3D size of order microns.

A complementary hypothesis is that condensin performs effectively two-sided extrusion facilitated by *in vivo* factors or conditions. In general, this can be achieved either via condensins that close unextruded gaps once bound to chromatin or via condensins that bind chromatin in a manner that inhibits the creation of gaps. A plausible mechanism of the first type of effectively two-sided extrusion is the switching mechanism. This model could be induced by subunit exchange [53], ambient conditions (e.g., concentration or ionic composition) [42], or protein modifications [60,61] not present in the single-molecule experiments. Another possibility is that LEFs extrude asymmetrically with speeds $v_1 > v_2$, in which case we would observe effectively two-sided extrusion if the slow side is fast enough to close gaps before disassociation (i.e., $v_2/k_u \gg d$) [65]. Yet another possibility is that *in vivo* factors or conditions enable actual two-sided loop extrusion, as it is described by previous models [17,20,21,23] but not observed *in vitro* [42].

Alternatively, LEFs could be effectively two-sided if condensins avoid creating gaps by dimerizing or otherwise cooperating or interacting to form two-sided complexes. This case could occur if condensins tend to associate at specific loading sites, randomly distributed loading complexes, or adjacent to other bound condensins [82–84]. However, high specificity would be needed in order to obtain the approximately 40-fold reduction in gap frequency needed for 1000-fold compaction [56]. Moreover, experimental evidence is consistent with uniform loading of condensins on mitotic chromosomes [8], and chromatid compaction can be achieved with condensin and a limited number of additional components [10,11], which suggests that loading factors are not necessary [14]. SMC complex oligomerization, however, is an alternative that is consistent with experimental observations for both condensin [85–87] and cohesin [88–90]. Such phenomena could generate effectively two-sided extrusion *in vivo* while allowing for the observation of one-sided extrusion *in vitro*. Future experiments could probe the conditions under which extrusion is two-sided *in vitro*.

Our theoretical model couples LEF loading and unloading kinetics with mean-field assumptions for the resulting loops. In this model, we find that steady-state linear compaction by pure one-sided loop extrusion is strictly limited. Consequently, current microscopic observations of one-sided loop extrusion by condensin [42] cannot explain macroscopic observations that condensins compact chromosomes into dense rodlike loop arrays [8,11]. Our findings thus raise the question of how condensins extrude loops *in vivo* to fully compact mitotic chromosomes. The model indicates that robust linear compaction for any type of LEF relies on minimizing the frequency of gaps of uncompacted chromatin [Eqs. (4) and (14)]. Thus, biological mechanisms that favor effectively two-sided loop extrusion, such as switching, cooperative binding, or dimerization, are likely necessary to achieve robust compaction of mitotic chromosomes. In particular, the model predicts that mammalian condensin complexes perform effectively two-sided loop extrusion under *in vivo* conditions.

ACKNOWLEDGMENTS

We thank Aafke van den Berg, Hugo Brandão, Anton Goloborodko, Maxim Imakaev, John Marko, Cees Dekker, Boris Khesin, and Kikuë Tachibana for helpful discussions and Johannes Nuebler for discussions and a critical reading of the manuscript. This work was supported by the NSF Physics of Living Systems (15049420), the NIH Polymer Models of Mitotic and Interphase Chromosomes (GM114190), and the NIH Center for 3D Structure and Physics of the Genome of the 4DN Consortium (DK107980).

[1] J. R. Paulson and U. K. Laemmli, *The Structure of Histone-Depleted Metaphase Chromosomes*, Cell **12**, 817 (1977).
[2] M. P. F. Marsden and U. K. Laemmli, *Metaphase Chromosome Structure: Evidence for a Radial Loop Model*, Cell **17**, 849 (1979).
[3] W. C. Earnshaw and U. K. Laemmli, *Architecture of Metaphase Chromosomes and Chromosome Scaffolds*, J. Cell Biol. **96**, 84 (1983).
[4] J. B. Lawrence, C. A. Villnave, and R. H. Singer, *Sensitive, High-Resolution Chromatin and Chromosome Mapping In Situ: Presence and Orientation of Two Closely Integrated Copies of EBV in a Lymphoma Line*, Cell **52**, 51 (1988).
[5] V. Guacci, E. Hogan, and D. Koshland, *Chromosome Condensation and Sister Chromatid Pairing in Budding Yeast*, J. Cell Biol. **125**, 517 (1994).
[6] K. Maeshima, M. Eltsov, and U. K. Laemmli, *Chromosome Structure: Improved Immunolabeling for Electron Microscopy*, Chromosoma **114**, 365 (2005).

[7] N. Naumova, M. Imakaev, G. Fudenberg, Y. Zhan, B. R. Lajoie, L. A. Mirny, and J. Dekker, *Organization of the Mitotic Chromosome*, Science **342**, 948 (2013).
[8] J. H. Gibcus, K. Samejima, A. Goloborodko, I. Samejima, N. Naumova, J. Neubler, M. Kanemaki, L. Xie, J. R. Paulson, W. C. Earnshaw, L. A. Mirny, and J. Dekker, *A Pathway for Mitotic Chromosome Formation*, Science **359**, 652 (2018).
[9] T. Hirano and T. J. Mitchison, *A Heterodimeric Coiled-Coil Protein Required for Mitotic Chromosome Condensation In Vitro*, Cell **79**, 449 (1994).
[10] K. Shintomi, T. S. Takahashi, and T. Hirano, *Reconstitution of Mitotic Chromatids with a Minimum Set of Purified Factors*, Nat. Cell Biol. **17**, 1014 (2015).
[11] K. Shintomi, F. Inoue, H. Watanabe, K. Ohsumi, M. Ohsugi, and T. Hirano, *Mitotic Chromosome Assembly Despite Nucleosome Depletion in Xenopus Egg Extracts*, Science **356**, 1284 (2017).
[12] T. Ono, A. Losada, M. Hirano, M. P. Myers, A. F. Neuwald, and T. Hirano, *Differential Contributions of Condensin I and Condensin II to Mitotic Chromosome Architecture in Vertebrate Cells*, Cell **115**, 109 (2003).
[13] T. R. Strick, T. Kawaguchi, and T. Hirano, *Real-Time Detection of Single-Molecule DNA Compaction and by Condensin I*, Curr. Biol. **14**, 874 (2004).
[14] T. Hirano, *Condensin-Based Chromosome Organization from Bacteria to Vertebrates*, Cell **164**, 847 (2016).
[15] A. D. Riggs, *DNA Methylation and Late Replication Probably Aid Cell Memory, and Type 1 DNA Reeling Could Aid Chromosome Folding and Enhancer Function*, Phil. Trans. R. Soc. B **326**, 285 (1990).
[16] K. Nasmyth, *Disseminating the Genome: Joining, Resolving, and Separating Sister Chromatids During Mitosis and Meiosis*, Annu. Rev. Genet. **35**, 673 (2001).
[17] E. Alipour and J. F. Marko, *Self-Organization of Domain Structures by DNA-Loop-Extruding Enzymes*, Nucleic Acids Res. **40**, 11202 (2012).
[18] J. F. Marko, P. De Los Rios, A. Barducci, and S. Gruber, *DNA-Segment-Capture Model for Loop Extrusion by Structural Maintenance of Chromosome (SMC) Protein Complexes*, Nucleic Acids Res. gkz497 (2019).
[19] C. Chapard, R. Jones, T. van Oepen, J. C. Scheinost, and K. Nasmyth, *Sister DNA Entrapment between Juxtaposed Smc Heads and Kleisin of the Cohesin Complex*, Mol. Cell **75**, 1 (2019).
[20] A. Goloborodko, M. V. Imakaev, J. F. Marko, and L. Mirny, *Compaction and Segregation of Sister Chromatids via Active Loop Extrusion*, eLife **5**, e14864 (2016).
[21] A. Goloborodko, J. F. Marko, and L. A. Mirny, *Chromosome Compaction by Active Loop Extrusion*, Biophys. J. **110**, 2162 (2016).
[22] A. L. Sanborn, S. S. P. Rao, S. C. Huang, N. C. Durand, M. H. Huntley, A. I. Jewett, I. D. Bochkov, D. Chinnappan, A. Cutkosky, J. Li, K. P. Geeting, A. Gnirke, A. Melnikov, D. McKenna, E. K. Stamenova, E. S. Lander, and E. L. Aiden, *Chromatin Extrusion Explains Key Features of Loop and Domain Formation in Wild-Type and Engineered Genomes*, Proc. Natl. Acad. Sci. USA **112**, E6456 (2015).
[23] G. Fudenberg, M. Imakaev, C. Lu, A. Goloborodko, N. Abdennur, and L. A. Mirny, *Formation of Chromosomal Domains by Loop Extrusion*, Cell Rep. **15**, 2038 (2016).
[24] G. Fudenberg, N. Abdennur, M. Imakaev, A. Goloborodko, and L. A. Mirny, *Emerging Evidence of Chromosome Folding by Loop Extrusion*, Cold Spring Harbor Symp. Quant. Biol. **82**, 45 (2018).
[25] C. A. Brackley, J. Johnson, D. Michieletto, A. N. Morozov, M. Nicodemi, P. R. Cook, and D. Marenduzzo, *Nonequilibrium Chromosome Looping via Molecular Slip Links*, Phys. Rev. Lett. **119**, 138101 (2017).
[26] C. A. Miermans and C. P. Broedersz, *Bacterial Chromosome Organization by Collective Dynamics of SMC Condensins*, J. Roy. Soc. Interace **15**, 20180495 (2018).
[27] J. R. Dixon, S. Selvaraj, F. Yue, A. Kim, Y. Li, Y. Shen, M. Hu, J. S. Liu, and B. Ren, *Topological Domains in Mammalian Genomes Identified by Analysis of Chromatin Interactions*, Nature (London) **485**, 376 (2012).
[28] E. P. Nora, B. R. Lajoie, E. G. Schulz, L. Giorgetti, I. Okamoto, N. Servant, T. Piolot, N. L. van Berkum, J. Meisig, J. Sedat, J. Gribnau, E. Barillot, N. Blüthgen, J. Dekker, and E. Heard, *Spatial Partitioning of the Regulatory Landscape of the X-Inactivation Centre*, Nature (London) **485**, 381 (2012).
[29] T. Sexton, E. Yaffe, E. Kenigsberg, F. Bantignies, B. Leblanc, M. Hoichman, H. Parrinello, A. Tanay, and G. Cavalli, *Three-Dimensional Folding and Functional Organization Principles of the Drosophila Genome*, Cell **148**, 458 (2012).
[30] S. S. P. Rao, M. H. Huntley, N. C. Durand, E. K. Stamenova, I. D. Bochkov, J. T. Robinson, A. L. Sanborn, I. Machol, A. D. Omer, E. S. Lander, and E. L. Aiden, *A 3D Map of the Human Genome at Kilobase Resolution Reveals Principles of Chromatin Looping*, Cell **159**, 1665 (2014).
[31] J. Gassler, H. B. Brandão, M. Imakaev, I. M. Flyamer, S. Ladstätter, W. A. Bickmore, J. M. Peters, L. A. Mirny, and K. Tachibana, *A Mechanism of Cohesin-Dependent Loop Extrusion Organizes Zygotic Genome Architecture*, EMBO J. **36**, 3600 (2017).
[32] W. Schwarzer, N. Abdennur, A. Goloborodko, A. Pekowska, G. Fudenberg, Y. Loe-Mie, N. A. Fonseca, W. Huber, C. H. Haering, L. Mirny, and F. Spitz, *Two Independent Modes of Chromatin Organization Revealed by Cohesin Removal*, Nature (London) **551**, 51 (2017).
[33] S. S. P. Rao *et al.*, *Cohesin Loss Eliminates All Loop Domains*, Cell **171**, 305 (2017).
[34] G. Wutz, C. Várnai, K. Nagasaka, D. A. Cisneros, R. R. Stocsits, W. Tang, S. Schoenfelder, G. Jessberger, M. Muhar, M. J. Hossain, N. Walther, B. Koch, M. Kueblbeck, J. Ellenberg, J. Zuber, P. Fraser, and J. M. Peters, *Topologically Associating Domains and Chromatin Loops Depend on Cohesin and Are Regulated by CTCF, WAPL, and PDS5 Proteins*, EMBO J. **36**, 3573 (2017).
[35] L. Vian *et al.*, *The Energetics and Physiological Impact of Cohesin Extrusion*, Cell **173**, 1165 (2018).
[36] X. Wang, T. B. K. Le, B. R. Lajoie, J. Dekker, M. T. Laub, and D. Z Rudner, *Condensin Promotes the Juxtaposition of DNA Flanking Its Loading Site in Bacillus Subtilis*, Genes Dev. **29**, 1661 (2015).
[37] N. T. Tran, M. T. Laub, and T. B. K. Le, *SMC Progressively Aligns Chromosomal Arms in Caulobacter Crescentus but Is Antagonized by Convergent Transcription*, Cell Rep. **20**, 2057 (2017).

[38] X. Wang, H. B. Brandão, T. B. K. Le, M. T. Laub, and D. Z. Rudner, *Bacillus Subtilis SMC Complexes Juxtapose Chromosome Arms as They Travel from Origin to Terminus*, Science **355**, 524 (2017).

[39] M. Hassler, I. A. Shaltiel, and C. H. Haering, *Towards a Unified Model of SMC Complex Function*, Curr. Biol. **28**, R1266 (2018).

[40] L. A. Mirny, M. Imakaev, and N. Abdennur, *Two Major Mechanisms of Chromosome Organization*, Curr. Opin. Cell Biol. **58**, 142 (2019).

[41] H. B. Brandão, X. Wang, P. Paul, A. A. van den Berg, D. Z. Rudner, and L. A. Mirny, *RNA Polymerases as Moving Barriers to Condensin Loop Extrusion*, bioRxiv, http://dx.doi.org/10.1101/604280 (2019).

[42] M. Ganji, I. A. Shaltiel, S. Bisht, E. Kim, A. Kalichava, C. H. Haering, and C. Dekker, *Real-Time Imaging of DNA Loop Extrusion by Condensin*, Science **360**, 102 (2018).

[43] T. Guérin, J. Prost, P. Martin, and J. F. Joanny, *Coordination and Collective Properties of Molecular Motors: Theory*, Curr. Opin. Cell Biol. **22**, 14 (2010).

[44] R. T. McLaughlin, M. R. Diehl, and A. B. Kolomeisky, *Collective Dynamics of Processive Cytoskeletal Motors*, Soft Matter **12**, 14 (2016).

[45] D. Saintillan, M. J. Shelley, and A. Zidovska, *Extensile Motor Activity Drives Coherent Motions in a Model of Interphase Chromatin*, Proc. Natl. Acad. Sci. USA **115**, 11442 (2018).

[46] R. K. Manna and P. B. S. Kumar, *Emergent Topological Phenomena in Active Polymeric Fluids*, Soft Matter **15**, 477 (2019).

[47] S. Ramaswamy, *The Mechanics and Statistics of Active Matter*, Annu. Rev. Condens. Matter Phys. **1**, 323 (2010).

[48] M. C. Marchetti, J. F. Joanny, S. Ramaswamy, T. B. Liverpool, J. Prost, M. Rao, and R. A. Simha, *Hydrodynamics of Soft Active Matter*, Rev. Mod. Phys. **85**, 1143 (2013).

[49] P. J. Foster, S. Fürthauer, M. J. Shelley, and D. J. Needleman, *From Cytoskeletal Assemblies to Living Materials*, Curr. Opin. Cell Biol. **56**, 109 (2019).

[50] T. Kruitwagen, P. Chymkowitch, A. Denoth-Lippuner, J. Enserink, and Y. Barral, *Centromeres License the Mitotic Condensation of Yeast Chromosome Arms*, Cell **175**, 780 (2018).

[51] T. Terakawa, S. Bisht, J. M. Eeftens, C. Dekker, C. H. Haering, and E. C. Greene, *The Condensin Complex Is a Mechanochemical Motor that Translocates along DNA*, Science **358**, 672 (2017).

[52] D. Gerlich, T. Hirota, B. Koch, J. M. Peters, and J. Ellenberg, *Condensin I Stabilizes Chromosomes Mechanically through a Dynamic Interaction in Live Cells*, Curr. Biol. **16**, 333 (2006).

[53] L. A. K. K. Borgmann, H. Hummel, M. H. Ulbrich, and P. L. Graumann, *SMC Condensation Centers in Bacillus Subtilis Are Dynamic Structures*, J. Bacteriol. **195**, 2136 (2013).

[54] N. Walther, M. J. Hossain, A. Z. Politi, B. Koch, M. Kueblbeck, Ø. Ødegård-Fougner, M. Lampe, and J. Ellenberg, *A Quantitative Map of Human Condensins Provides New Insights into Mitotic Chromosome Architecture*, J. Cell Biol. **217**, 2309 (2018).

[55] In particular, as can be obtained from subsequent calculations, this interpretation of $\mathcal{FC}$ is true for $L/d > \{\ln[(1-\alpha)^{-1}]+1\}f/(1-f)$. For pure one-sided extrusion, this is $L/d > 20.4$. For mammalian chromosomes *in vivo*, we expect $L/d \approx 10^3$–10^4 [54,58,59]. Thus, this interpretation of $\mathcal{FC}$ holds for pure one-sided extrusion in physiological scenarios. For the model with both one-sided and two-sided extruders, this range of L/d corresponds to upper bounds on ϕ in the range of 0.70–0.87.

[56] See Supplemental Material at http://link.aps.org/supplemental/10.1103/PhysRevX.9.031007 for (I) theory for compaction with out unbinding, (II) discussion of finite-size effects in simulations, (III) details of the theory in the sparse regime, (IV) analysis of the model with biased loading, and (V) a Supplemental figure showing the mean gap size in simulations.

[57] Since Eq. (7) fixes the number of LEFs per loop, it also fixes the total fraction of parent LEFs, N_p/N.

[58] A. Takemoto, K. Kimura, S. Yokoyama, and F. Hanaoka, *Cell Cycle-Dependent Phosphorylation, Nuclear Localization, and Activation of Human Condensin*, J. Biol. Chem. **279**, 4551 (2004).

[59] K. Fukui and S. Uchiyama, *Chromosome Protein Framework from Proteome Analysis of Isolated Human Metaphase Chromosomes*, Chem. Rec. **7**, 230 (2007).

[60] M. Kschonsak, F. Merkel, S. Bisht, J. Metz, V. Rybin, M. Hassler, and C. H. Haering, *Structural Basis for a Safety-Belt Mechanism that Anchors Condensin to Chromosomes*, Cell **171**, 588 (2017).

[61] A. M. O. Elbatsh, J. A. Raaijmakers, R. H. van der Weide, J. uit de Bos, H. Teunissen, S. Bravo, R. H. Medema, E. de Wit, C. H. Haering, and B. D. Rowland, *Condensin's ATPase Machinery Drives and Dampens Mitotic Chromosome Condensation*, bioRxiv, http://dx.doi.org/10.1101/216630 (2017).

[62] D. Gerlich, B. Koch, F. Dupeux, J. M. Peters, and J. Ellenberg, *Live-Cell Imaging Reveals a Stable Cohesin-Chromatin Interaction after but not before DNA Replication*, Curr. Biol. **16**, 1571 (2006).

[63] J. Stigler, G. Ö. Çamdere, D. E. Koshland, and E. C. Greene, *Single-Molecule Imaging Reveals a Collapsed Conformational State for DNA-Bound Cohesin*, Cell Rep. **15**, 988 (2016).

[64] A. S. Hansen, I. Pustova, C. Cattoglio, R. Tjian, and X. Darzacq, *CTCF and Cohesin Regulate Chromatin Loop Stability with Distinct Dynamics*, eLife **6**, e25776 (2017).

[65] E. J. Banigan, A. van den Berg, H. B. Brandão, J. F. Marko, and L. A. Mirny (work in progress).

[66] K. C. Palozola, G. Donahue, H. Liu, G. R. Grant, J. S. Becker, A. Cote, H. Yu, A. Raj, and K. S. Zaret, *Mitotic Transcription and Waves of Gene Reactivation During Mitotic Exit*, Science **358**, 119 (2017).

[67] O. Cuvier and T. Hirano, *A Role of Topoisomerase II in Linking DNA Replication to Chromosome Condensation*, J. Cell Biol. **160**, 645 (2003).

[68] K. Nagasaka, M. J. Hossain, M. J. Roberti, J. Ellenberg, and T. Hirota, *Sister Chromatid Resolution Is an Intrinsic Part of Chromosome Organization in Prophase*, Nat. Cell Biol. **18**, 692 (2016).

[69] M. Takahashi, T. Wakai, and T. Hirota, *Condensin I-Mediated Mitotic Chromosome Assembly Requires Association with Chromokinesin KIF4A*, Genes Dev. **30**, 1931 (2016).

[70] O. V. Borisov and A. Halperin, *Micelles of Polysoaps*, Langmuir **11**, 2911 (1995).
[71] J. F. Marko, *Linking Topology of Tethered Polymer Rings with Applications to Chromosome Segregation and Estimation of the Knotting Length*, Phys. Rev. E **79**, 051905 (2009).
[72] V. F. Scolari and M. C. Lagomarsino, *Combined Collapse by Bridging and Self-Adhesion in a Prototypical Polymer Model Inspired by the Bacterial Nucleoid*, Soft Matter **11**, 1677 (2015).
[73] B. J. Trask, S. Allen, H. Massa, A. Fertitta, R. Sachs, G. Van den Engh, and M. Wu, *Studies of Metaphase and Interphase Chromosomes Using Fluorescence in situ Hybridization*, Cold Spring Harbor Symp. Quant. Biol. **58**, 767 (1993).
[74] S. Brahmachari and J. F. Marko, *Chromosome Disentanglement Driven via Optimal Compaction of Loop-Extruded Brush Structures*, bioRxiv, http://dx.doi.org/10.1101/616102 (2019).
[75] T. M. Birshtein, O. V. Borisov, Y. B. Zhulina, A. R. Khokhlov, and T. A. Yurasova, *Conformations of Comb-like Macromolecules*, Polym. Sci. USSR **29**, 1293 (1987).
[76] G. H. Fredrickson, *Surfactant-Induced Lyotropic Behavior of Flexible Polymer Solutions*, Macromolecules **26**, 2825 (1993).
[77] Y. Rouault and O. V. Borisov, *Comb-Branched Polymers: Monte Carlo Simulation and Scaling*, Macromolecules **29**, 2605 (1996).
[78] J. Paturej, S. S. Sheiko, S. Panyukov, and M. Rubinstein, *Molecular Structure of Bottlebrush Polymers in Melts*, Sci. Adv. **2**, e1601478 (2016).
[79] S. S. Sheiko, O. V. Borisov, S. A. Prokhorova, and M. Möller, *Cylindrical Molecular Brushes under Poor Solvent Conditions: Microscopic Observation and Scaling Analysis*, Eur. Phys. J. E **13**, 125 (2004).
[80] N. G. Fytas and P. E. Theodorakis, *Molecular Dynamics Simulations of Single-Component Bottle-Brush Polymers with Flexible Backbones under Poor Solvent Conditions*, J. Phys. Condens. Matt. **25**, 285105 (2013).
[81] We expect nucleosomes to introduce an order 1 factor. Nucleosomes contain approximately 150 bp and have a diameter of approximately 10 nm. The resulting fiber has an estimated persistence length of a few nucleosomes.
[82] Y. Frosi and C. H. Haering, *Control of Chromosome Interactions by Condensin Complexes*, Curr. Opin. Cell Biol. **34**, 94 (2015).
[83] X. Robellet, V. Vanoosthuyse, and P. Bernard, *The Loading of Condensin in the Context of Chromatin*, Curr. Genet. **63**, 577 (2017).
[84] A. S. Cacciatore and B. D. Rowland, *Loop Formation by SMC Complexes: Turning Heads, Bending Elbows, and Fixed Anchors*, Curr. Opin. Genet. Dev. **55**, 11 (2019).
[85] S. H. Yoshimura, K. Hizume, A. Murakami, T. Sutani, K. Takeyasu, and M. Yanagida, *Condensin Architecture and Interaction with DNA: Regulatory Non-SMC Subunits Bind to the Head of SMC Heterodimer*, Curr. Biol. **12**, 508 (2002).
[86] H. Barysz, J. H. Kim, Z. A. Chen, D. F. Hudson, J. Rappsilber, D. L. Gerloff, and W. C. Earnshaw, *Three-Dimensional Topology of the SMC2/SMC4 Subcomplex from Chicken Condensin I Revealed by Cross-Linking and Molecular Modelling*, Open Biol. **5**, 150005 (2015).
[87] R. A. Keenholtz, T. Dhanaraman, R. Palou, J. Yu, D. D'amours, and J. F. Marko, *Oligomerization and ATP Stimulate Condensin-Mediated DNA Compaction*, Sci. Rep. **7**, 14279 (2017).
[88] N. Zhang, S. G. Kuznetsov, S. K. Sharan, K. Li, P. H. Rao, and D. Pati, *A Handcuff Model for the Cohesin Complex*, J. Cell Biol. **183**, 1019 (2008).
[89] T. Eng, V. Guacci, and D. Koshland, *Interallelic Complementation Provides Functional Evidence for Cohesin-Cohesin Interactions on DNA*, Mol. Biol. Cell **26**, 4224 (2015).
[90] C. Cattoglio, I. Pustova, N. Walther, J. J. Ho, M. Hantsche-Grininger, C. J. Inouye, M. J. Hossain, G. M. Dailey, J. Ellenberg, X. Darzacq, R. Tjian, and A. S. Hansen, *Determining Cellular CTCF and Cohesin Abundances to Constrain 3D Genome Models*, eLife **8**, e40164 (2019).